RSC Advances

ROYAL SOCIETY OF CHEMISTRY

www.rsc.org/advances

Self-cleaning SiO_x-embedded TiO_2/SiO_2 alternating multilayer

Soon Wook Kim,[a] Nguyen Tri Khoa,[a] Doan Van Thuan,[a] Eui Jung Kim*[b] and Sung Hong Hahn*[a]

Received 00th January 20xx,
Accepted 00th January 20xx

DOI: 10.1039/x0xx00000x

www.rsc.org/

A new system that inserts an eco-sustainable and hydrophilic system into an anti-reflection (AR) system was developed and identified the applicability to the photovoltaic system. We assembled TiO_2 nanoparticle composite with the densely multi-layered AR system as a top layer to show the eco-sustainable, hydrophilic performances and play a role of the low refractive index material which is essential for AR. The hydrophilic system displayed the lowest reflectance and remarkable reduction of the contact angle to 0 degree under UV light irradiation. The annealed hydrophilic system (eco-sustainable system) exhibited the highest photodecomposition activity of 100 % within 90 min by the effective separation of electron-hole pairs using SiO_x nanoparticles inside of TiO_2 layer as the trap levels. This successful AR, hydrophilic, and eco-sustainable performances with the simplified system using only two materials of TiO_2, SiO_x are absotively anticipated to contribute to the enhancement of photovoltaic system efficiency.

1. Introduction

In recent years, transition metal oxide materials (TMOM) have been paid much attention due to their remarkable optical properties in anti-reflection (AR) and photocatalytic applications. AR systems are used in photovoltaic devices to improve the absorption efficiency of solar irradiation. On the other hand, photocatalytic systems, which have been greatly attracted in environmental purification, are called eco-sustainable systems and received much attention due to a large number of recent worldwide environmental problems. So far, AR and eco-sustainable researches have had the characteristic of being contradictory, as most studies were separately focused on characterization and fabrication of either AR or eco-sustainable systems. Combination of the two systems is expected to enlarge the applied areas of TMOM.

AR system is an optical thin film utilized for increasing optical transmission rate of substrate. It is a method for reducing reflection by using the interference effect of light generated by the refractive index differences between thin-film and substrate. Such systems have been widely used in liquid crystal display, plasma display panel, light-emitting diode, organic electroluminescence, including display optical element, optical filter, solar cell, and other applications.[1-4] Generally, by using materials with high (H), low (L), and middle (M) refractive index, a multilayer AR coating with high transmittance in a wide visible wavelength range can be realized. In the AR coating design for a wide wavelength range, there are three common methods employed: The first is the W-coating (air/LHH/glass), the second is the quarter-half-quarter coating (air/LHHM/glass), and the last is the multilayer AR coating (air/LHH0.32L0.26H /glass).[5] The key feature of these three methods is that a low refractive index material is used in the first layer in order to reduce reflection because a high refractive index material shows high reflectance.

The eco-sustainable system of photocatalytic performance recently attracted much attention due to their various applications in environmental purification and dye sensitized photovoltaic solar cells. Among various metal oxide photocatalysts, titanium oxide (TiO_2) has been one of the most promising materials in both fundamental studies and practical applications because of its high photoactivity, biological and chemical inertness, cost effectiveness, non-toxicity, and long-term stability against photo-corrosion and chemical corrosion.[6-8] Upon band-gap excitation of TiO_2, the photo-induced electrons and positively charged holes can reduce and oxidize the species adsorbed on the surface of TiO_2 particles, respectively.[9-12] Metal-doped TiO_2 can reduce the electron–hole pairs recombination and increase the hydroxyl radical concentration on TiO_2 surface, resulting in an increased photocatalytic activity of TiO_2 thin film.[13,14] Although many researches have been carried out to enhance the efficiency of a photovoltaic device, there are chronic and environmental troubles caused by dust and contaminants on the surface of the device. Photovoltaic systems are generally located in an outdoor area and exposed to many pollutants which results in reduction of solar transmittance.[15] To protect the systems from dust and contaminants, many researchers focus on self-cleaning effect and hydrophilicity is one of the solutions for that. The hydrophilic surface causes the water to be flat and then this water cleans the dust and contaminants on the surface because of its sliding down by gravity.[16]

In this article, we applied TiO_2 nanoparticle composite on the multi-layer AR thin film to actualize a novel eco-sustainable AR (E-AR) and a hydrophilic AR (H-AR) system and tried to demonstrate the mechanism by investigating the refractive index, crystallinity, and distribution of SiO_x material in TiO_2 layers. Reflectance and transmittance were analyzed to evaluate the AR effect; water contact angle and photodecomposition of methylene blue under black-light irradiation were measured to confirm the hydrophilic and the eco-sustainable effects, respectively.

2. Results and discussion

We prepared the traditional AR (T-AR) system of $SiO_2/TiO_2/SiO_2/TiO_2$ multi-layer and the hydrophilic AR (H-AR) system which introduce TiO_2 nano-sphere (L-TiO_2) layer on T-

[a] Department of Physics and Energy Harvest-Storage Research Center, University of Ulsan, Ulsan 680-749, South Korea.
E-mail: shhahn@ulsan.ac.kr; Fax: +82 52 259 1693; Tel: +82 52 259 2330
[b] Department of Chemical Engineering, University of Ulsan, Ulsan 680-749, South Korea.
E-mail: ejkim@ulsan.ac.kr; Fax: +82 52 259 1689; Tel: +82 52 259 2832

AR system (Fig. 1a). TiO_2 nano-sphere was developed using glancing angle deposition and reduced its refractive index to be less than 1.500 at 550 nm similar to SiO_2 thin film as shown in Fig. 1a. A low refractive index nano-sphere TiO_2 (L-TiO_2) layer was fixed with 10 nm thickness and the optimization process was carried out using the thin-film design software Essential Macleod. The refractive index of TiO_2, L-TiO_2, and SiO_2 layers of H-AR system is found to be 2.365, 1.498, and 1.487 at 550 nm of reference wavelength, respectively (Fig. 1b). The refractive index of L-TiO_2 is conspicuously reduced and nearly equal to that of SiO_2. This shows the possibility of simultaneous manifestation of AR and photocatalytic activity with only one system by substitution L-TiO_2 for SiO_2. The reflectance values of T-AR and H-AR systems are shown in Fig. 1c. The average reflectance in the visible light range (400-700 nm) is reduced to 0.90 % and 0.35 % for T-AR system and H-AR system, respectively. The average transmittance of these systems, considered the backside surface effect of substrate,[17] is over 95 %. Fig. 1d shows the change of transient water-contact-angle on T-AR system, L-TiO_2 thin film, and H-AR system under UV light irradiation. T-AR system shows a slight loss of 5 and L-TiO_2 system drops the angle to 20 in 80 min. But, in the case of H-AR system, it displays extraordinary reduction to 0 in only 40 min. L-TiO_2 adopted system shows a remarkable decrease of contact angle value and this can be explained with the metastable OH groups produced by the interaction of hole and H_2O molecular under UV light irradiation. These OH radicals generated from the photoinduced reaction, are thermodynamically less stable and increase the surface energy of the TiO_2 that result in the hydrophilic modification.[18] The best result is obtained from H-AR system which has a SiO_2 layer under L-TiO_2 nanoparticles. This result corresponds with chemical changes of the surface structure and increase of hydroxyl groups at the interfaces by enhancing acidity of the Si-O-Ti bonds by UV light irradiation.[19]

Fujishima et al.[20] studied about the hydrophilic conversion of TiO_2 surface and demonstrated that the hydrophilic conversion phenomenon can be explained by photocatalytic oxidation and metastable state. The metastable state is caused by an increase in the number of OH groups on the TiO_2 surface which has high surface energy. A highly hydrophilic conversion was completed even if stains remained on the surface and it retained that condition for a day or two under the ambient condition without additional light irradiation. After several days, it returned to the initial hydrophobic condition. They predicted the hydrophilic and hydrophobic conversions of the H-AR system. The E-AR system can be obtained with various conditions such as light irradiation and dark condition. The rate of conversion between H-AR and E-AR depends on the number of OH groups. The E-AR system may exhibit faster hydrophilic conversion and slower hydrophobic conversion rate.

E-AR system was prepared by annealing H-AR system at 650 °C for 30 min (Fig. 2a). During heat treatment, the thin film becomes dense due to the reduction of voids and it results in the decrease of its optical thickness. Therefore, in this work, we prepared dense films through the evaporation process[21] so that the change of layer structure is minimized during the annealing process. It is shown that the changes in optical property according to the modification of thin film phase are minimized through the preceding research regarding the dense TiO_2 thin-film. The transmittance spectra of H-AR and E-AR systems show that they have similar transmittance in the visible range (Fig. 2b, c). Slight changes in optical transmittance result from small differences of refractive index due to the film densification. E-AR system and H-AR system have an average transmittance value of about 95.76 % and 95.95 % in the range of 400 to 700 nm, respectively. Thus we can expect their reflectance to be below 1.00 % in the visible range.

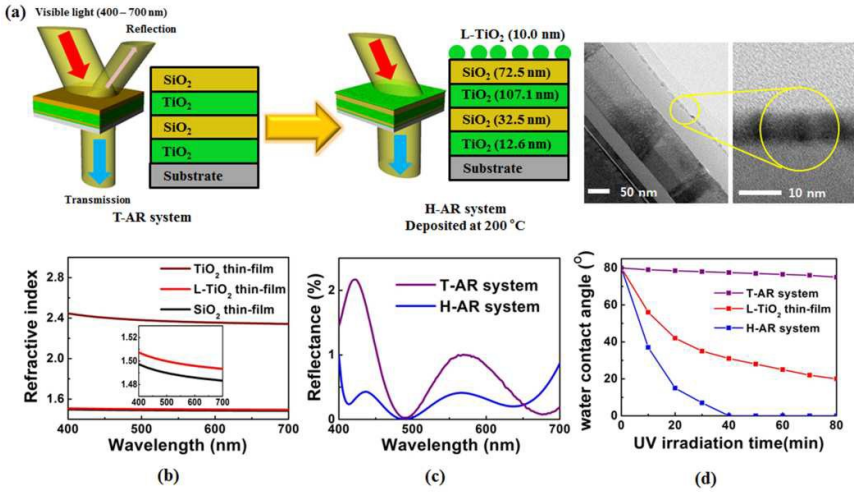

Figure 1. (a) The schematic diagram and the cross-sectional STEM-HAADF image of H-AR systems. (b) The refractive indices of the TiO_2, L-TiO_2, and SiO_2 thin-films in the visible range. (c) The reflectance of T-AR system and H-AR system. (d) Photo-induced reduction of the water-contact-angle of T-AR system, L-TiO_2 thin film, and H-AR system.

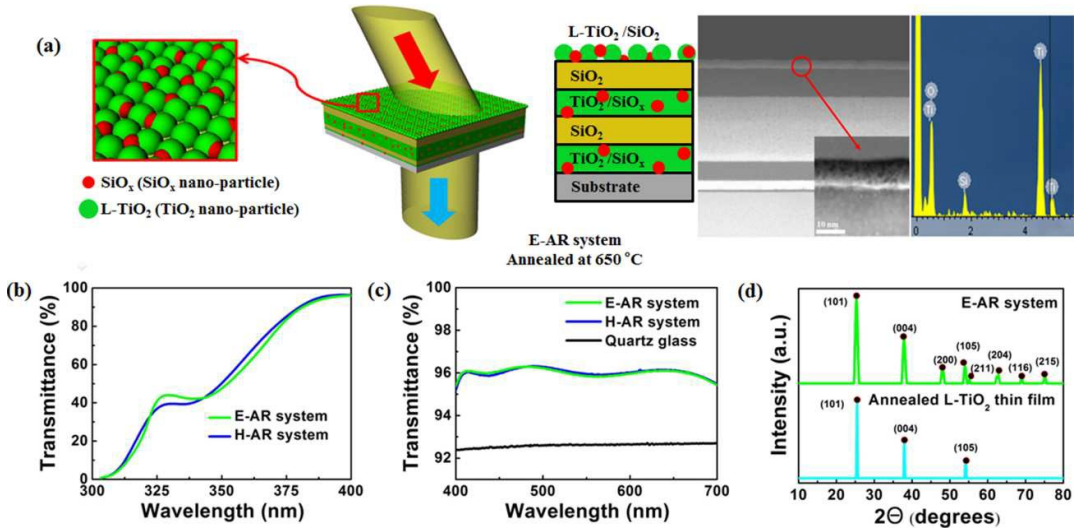

Figure 2. (a) The schematic diagram of post-annealed H-AR (E-AR) systems, the HR-TEM images, and the EDS analysis of L-TiO_2 top layer. (b, c) The transmittance of E-AR system, H-AR system, and quartz glass. (d) The X-ray diffraction patterns of L-TiO_2 top layer of E-AR system and L-TiO_2 thin-film annealed at 650°C.

Table1. The EDS results of E-AR system

Layers	O	Si	Ti
1	60.71	5.67	33.62
2	62.63	37.37	
3	54.98	5.37	39.65
4	54.51	45.49	
5	55.73	6.68	37.59

There is a sudden decrease in transmittance blow 400 nm, meaning that a UV light is absorbed by the AR coating. This UV absorption is favorable to photocatalytic performance under black light irradiation but unfavorable to solar cell current. (Fig. 2b) Although the AR coating has a disadvantage of UV absorption, it has a more attractive benefit of visible light transmittance.

Yu et al. investigated the effect of nanocone arrays as an antireflective coating on the device performance of a solar cell. Although the film coated with nanocone arrays shows a decreased transmittance below 350 nm, it exhibits a higher transmittance than uncoated film in the range of 400 to 1800 nm, which enhances the device efficiency.[16]

Figure 2a shows a schematic diagram of the E-AR system. The chemical composition of particles was determined by energy dispersive spectroscopy (EDS). (Table 1) The EDS spectrum indicated that the amorphous particles have Si-O bonding. According to the EDS results, Si-O bonding particles have a stoichiometry of SiO_2 during the annealing process. Since SiO_2 particles are smaller than TiO_2 particles, the diffusion of SiO_2 particles (or Ti and Si in the oxide matrix) occurs throughout TiO_2 particles, which is activated by thermal energy.[22]

Figure 2d shows the X-ray diffraction patterns of L-TiO_2 top layer of E-AR system and annealed L-TiO_2 thin-film deposited on quartz glass to compare the differences according to the exist of SiO_2 layer under L-TiO_2 layer or not. The crystallite sizes of anatase TiO_2 of E-AR system and annealed L-TiO_2 thin film are 12.5 and 18.7 nm, respectively. SiO_2 under-layer seemed to suppress the single crystallization of anatase phase. Consequently, due to SiO_2 under-layer, the anatase phase peak of E-AR system revealed a smaller crystallite size as compared to annealed L-TiO_2 thin film.

Figure 3 shows the surface morphology of the AR system. The surface of the H-AR system (before heat treatment) was composed of spherical TiO_2 particles, while the surface of the E-AR (after heat treatment) consisted with non-spherical particles as a result of phase transform to anatase with embedding of SiO_x and agglomeration of particles.

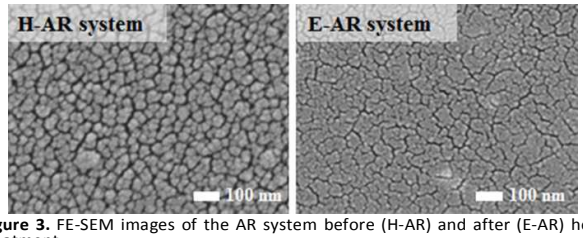

Figure 3. FE-SEM images of the AR system before (H-AR) and after (E-AR) heat treatment.

The surface characterizations of E-AR system and H-AR system were obtained by X-ray photoelectron spectroscopy (XPS) as shown in Fig. 4a and b. The C1s photoelectron peak is shown at 284.60 eV, which may come from the carbon pollution in air or the remaining organic components. Fig. 4a shows the expanded spectrum of O1s photoelectron peak, which was fitted into three peaks by Lorentzian curves appearing at 532.5 eV, 531.6 eV, and 530.1 eV, and can be attributed to Si–O–Si, Si–O–Ti, and Ti–O–Ti components, respectively.[23] The XPS results show that more complicated oxygen coordination states appear in E-AR system than in H-AR system, and that more connections are present between titanium species and the silica matrix. Furthermore, the oxidation states of Ti element in L-TiO_2 top layer of E-AR system for $Ti^{3+}2p$ ($Ti^{3+}2p_{1/2}$ at 462.35 eV, $Ti^{3+}2p_{3/2}$ at 456.51 eV) peaks and $Ti^{4+}2p$ ($Ti^{4+}2p_{1/2}$

at 463.98 eV, $Ti^{4+}2p_{3/2}$ at 458.21 eV) peaks were detected as reported previously.[24] The XPS spectrum of Si2p core electrons for L-TiO_2 top layer clearly matches the EDS measurement for amorphous particles with Si-O bonding in Fig. 2d; the measured binding energy is 101.6 eV, which is a typical value for SiO_x species.[25] Moreover, SiO_x species were formed by Ti-O-Si bonding on the surface of E-AR system through heat treatment. The formation process of SiO_x species can be explained as follows. Ti-O-Si bonding is formed due to the coexistence of TiO_2 and TiO_x by electron beam effect. SiO_2 particle moves into TiO_2 layers by the annealing effect and SiO_2 bonding particles interact with TiO_x bonding particles in top layer by thermal energy. As the binding energy of Ti-O bonding is stronger than that of Si-O bonding, the amount of Ti^{3+} is reduced during the thermal process, so SiO_x species is formed. We can confirm this process by comparing O 1s peaks and Ti2p peaks in Fig. 4a-b. In Fig. 4b, the spectrum of pure L-TiO_2 contains one peak appearing at 529.5 eV, which is typical for metal oxides and agrees with O 1s electron binding energy for TiO_2 molecules. In the XPS narrow scan spectrum of $Ti^{3+}2p$ ($Ti^{3+}2p_{1/2}$ at 462.36 eV, $Ti^{3+}2p_{3/2}$ at 457.02 eV) peaks and $Ti^{4+}2p$ ($Ti^{4+}2p_{1/2}$ at 464.26 eV, $Ti^{4+}2p_{3/2}$ at 458.73 eV) peaks were detected. The observation of the Ti^{3+} state on TiO_2 surface is important. Because, it can play a role as a metal or doped impurity, which can capture the reaction electrons, remaining unpaired charges, and support photocatalytic activity. The X-ray photoelectron spectrum of Si 2p core electrons was not observed in H-AR system.

Bard et al.,[26] demonstrated the usefulness of TiO_2/SiO_2 multilayer. TiO_2 has pholyphases, such as anatase, rutile, brookite phase depending on annealing temperature. In the case of the TiO_2/SiO_2 layer system, the SiO_2 lattice locks the Ti-O species at the interface preventing the nucleation which is necessary for the phase transformation to rutile. As a result, TiO_2/SiO_2 mixed layer shows more anatase phase than TiO_2 single layer at the same annealing temperature. It is known that the anatase phase of TiO_2 has good catalytic performance. Accordingly, the TiO_2/SiO_2 layer is expected to show more effective photocatalytic performance than TiO2 single layer.

PL spectra of E-AR system and annealed L-TiO_2 thin film at room temperature are shown in Fig. 4c and d. A peak at 385 nm corresponds to the near-band-edge emission of TiO_2 and emissions at 405 nm, 421 nm, and 426 nm may be attributed to the radiative recombination at the donor levels caused by Ti^{3+} ions.[27] An energy-level diagram in Fig. 4c shows that emissions at 450 and 475 nm are possibly related to two trap levels of the SiO_x-embedded TiO_2 particles.

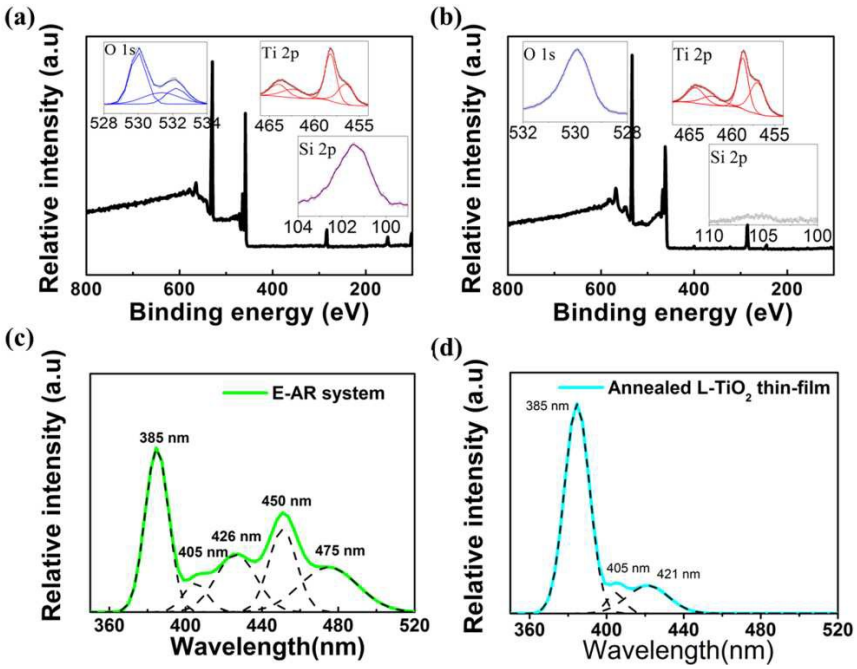

Figure 4. X-ray photoelectron spectra of top layer of (a) E-AR system and (b) H-AR system. The PL spectra of (c) E-AR system and annealed (d) L-TiO_2 thin film.

The photocatalytic activity of the prepared samples was evaluated by measuring the photodegradation rates of methylene blue (MB) under UV irradiation. The photodegradation rate is calculated by the following equation: photodegradation rate = C/C_0 where C_0 is the initial concentration of MB and C is the MB concentration at a given time. The MB degradation with the UV irradiation time for E-AR system, H-AR system, L-TiO_2 thin-film, annealed L-TiO_2 thin film, and the MB self-photofading is depicted in Fig 5. It is clearly demonstrated that E-AR system achieves the best performance for MB photodegradation. The MB pollutant is almost completely decomposed after 90 min. However, only about 38 % and 61 % of MB dye is removed after 300 min by H-AR system and annealed L-TiO_2 thin film, respectively. In the case of L-TiO_2 thin film, the increased photodegradation rate

after heat treatment is attributed to crystallization of TiO_2 to anatase phase.

An enhancement in photocatalytic activity of E-AR system by SiO_x-embeded TiO_2 can be explained as follows. As shown in the schematic diagram of Fig. 5b, conduction band (CB) and valence band (VB) edges of TiO_2 and SiO_x-embeded TiO_2 are located with trap levels. Under UV irradiation, the electron-hole pairs are initially generated in TiO_2 and SiO_x-embeded TiO_2. The generated electrons are accumulated in CB and attracted to trap levels due to the difference in work functions, thus preventing e^--h^+ recombination. The generated holes (h^+) react with H_2O and OH^- groups adsorbed on TiO_2 surface to produce hydroxyl radicals. The electrons accumulated in trap levels of SiO_x-embeded TiO_2 reunite with the holes that are unreacted with water. The PL spectra of E-AR system and annealed L-TiO_2 thin film in Fig. 4c and d suggest that there are two trap levels located at 2.76 eV (450 nm), 2.61 eV (475 nm) above the VB of TiO_2. Consequently, the excellent photocatalytic activity of E-AR system is attributed to SiO_x-embeded TiO_2 nanoparticles produced in the heat treatment process.

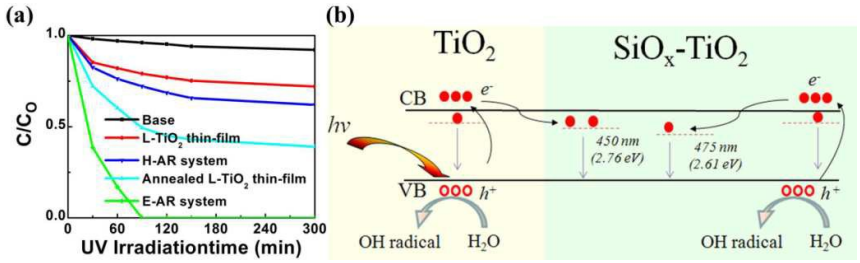

Figure 5. (a) The photocatalytic activities of samples evaluated by the photodegradation of methylene blue in aqueous solution. (b) The Energy-level diagram of E-AR system showing the Fermi level of TiO_2 and trap levels of SiO_x-embedded TiO_2 contacts.

3. Experimental

The samples were prepared on quartz substrates using a high-vacuum e-beam evaporation system (SHT-CT-800A-DA, Korea). The evaporation sources were periodically shuttered via computer controlled pneumatic shutters with 7.0 kV of electron gun voltage. The current was controlled at 220 mA for TiO2 and 110 mA for SiO_2. The sources of TiO_2 and SiO_2 were 99.99 % pure.

To prepare a more densified film, the electron beam evaporator was evacuated to 6.0×10^{-6} torr of base pressure; TiO_2 and SiO_2 films were deposited at 200 °C. The partial pressure of oxygen gas was 6.0×10^{-5} torr for TiO_2 film deposition and 5.0×10^{-5} torr for SiO_2 film deposition. Oxygen was introduced during the deposition using a mass flow controller (MKS 1179A) to promote the growth of a more stoichiometric film at an oxygen partial pressure of 5.0×10^{-5} torr. In the case of insufficient oxygen, a stoichiometric film was made by the effect of the electron beam radiation. The substrates were rotated at 15 rpm to obtain uniform films. TiO_2 and SiO_2 thin films were deposited at rates of 2.5 Å/s and 7.0 Å/s, respectively.

We fabricated the low-refractive index of TiO_2 top layer by application of nano-sphere layer. The nano-sphere layer was prepared by glancing angle deposition. L-TiO_2 film was fabricated with incident vapor flux at an angle of 72° relative to substrate, a deposition rate of 2.0 Å/s, and no substrate rotation.

The phase of TiO_2 is changed from anatase to rutile in the annealing process. According to our previous study, anatase and rutile phases of TiO_2 thin film are formed at 400 and 800 °C, respectively. TiO_2 thin film is amorphous below 400 °C and undergoes morphological and optical changes such as an increase in grain size and a decrease in transmittance above 700°C.[28] A wide variation of grain size leads to the defects between TiO_2 and SiO_2 interfaces and a decreased film transmittance results in a reduced efficiency of the photovoltaic system. So, we slowly raised the annealing temperature to 650 °C at a rate of 10 °C/min to prevent problems mentioned above and maintained that temperature for 30 min under atmosphere. The sample was then allowed to cool naturally.

The optical constant of the thin films was evaluated by spectroscopic ellipsometry (Ellipsotech, Elll–SE–F). The hydrophilicity of the films surface was quantified from water contact angle measurements. Experiments were performed at room temperature in air using a goniometer equipped with a digital camera. Several water droplets (0.5 µL) were spread on the samples and water contact angles were measured under irradiation of four surrounding 20 W black-light (UVA) lamps (wavelength range: 315-400 nm). Each lamp was located at the side of a square box and it was 10 cm away from the sample. The optical transmittance of systems was measured with a HP 8453 spectrophotometer. The crystal phase of samples was determined by X-ray diffraction (XRD, Philips PW3710) in the 2θ mode using monochromatic Cu Kα radiation at 30 kV and 20 mA. The θ range used in XRD measurements was from 20° to 80° in steps of 0.02° s^{-1}. In order to investigate nanostructure, high angle annular dark field (HAADF-STEM) imaging was applied for observing L-TiO_2 layer using JEM-2200FS. To evaluate the compositional variation of L-TiO_2 layer, high resolution transmission electron microscopy (HR-TEM) and energy dispersive spectroscopy (EDS) were also applied using JEM-2200FS. The surface chemical state of elements was analyzed by X-ray photoelectron spectroscopy

(XPS, KBSI, ESCALAB 250) with a monochromatic Al Kα X-ray source. The photocatalytic properties of samples were performed by measuring the photodecomposition of MB ($C_{16}H_{18}N_3S$-Cl-$3H_2O$) with initial concentration of 10^{-5} mol/L under irradiation of four surrounding 20 W-black-light (UVA) lamps (wavelength range: 315-400 nm). Photocatalytic degradation was monitored by measuring the absorption spectra of solution at λ_{max} = 664 nm. Photoluminescence (PL) spectra were collected on Cary Eclipse fluorescence spectrophotometer (Varian) with 295 nm of excitation wavelength.

4. Conclusions

The hydrophilic, photocatalytic, and AR properties have been successfully realized in one facile system of TiO_2 and SiO_2 by controlling the morphology of top layer and heat treatment. The low refractive index nano-sphere TiO_2 (L-TiO_2) layer facilitates the multi-layer system to have considerable optical properties and extraordinary hydrophilicity under the UV light irradiation. The heat treatment at 650 °C leads to the specific chemical bonding changes and displays an effective separation of photogenerated electron and hole pairs by formation of trap levels between conduction band and valence band. This functionalized system showed a remarkable photocatalytic activity of 100 % within 90 min and revealed the high potential for the improvement of photovoltaic system efficiency.

Acknowledgements

This research was financially supported by Priority Research Centers Program (2009-0093818) and by the National Research Foundation of Korea (NRF) through the Basic Science Research Program (2012R1A1A4A01015466).

References

1 J. K. Kim, T. Gessmann, E. F. Schubert, J. Q. Xi, H. Luo, J. Cho, C. Sone and Y. Park, *Appl. Phys. Let.,* 2006, **88**, 013501.
2 N. Wang, J. Fang, X. Zhang, G. Wang, L. Wang, C. Liu, H. Zhao, Z. Chen, X. L. Chen, J. Sun and Y. Zhao, *Sol. Energ. Mat. Sol. C.,* 2014, **130**, 420.
3 Y. Wang, H. Wang, X. Meng and R. Chen, *Sol. Energ. Mat. Sol., C.* 2014, **130**, 71.
4 T. Glaser, A. Ihring, W. Morgenroth, N. Seifert, S. Schroter and V. Baier, *Microsyst. Technol.,* 2005, **11**, 86.
5 H. A. Macleod, *Thin-Film Optical Filters 2nd edn,* Hilger, 1986.
6 H. S. Kim, J. W. Lee, N. Yantara, P. P. Boix, S. A. Kulkarni, S. Mhaisalkar, M. Grätzel and N.G. Park, *Nano Let.,* 2013, **13**, 2412.
7 L. Etgar, D. Yanover, R. K. Čapek, R. Vaxenburg, Z. Xue, B. Liu, M. K. Nazeeruddin, E. Lifshitz and M. Grätzel, *Adv. Funct. Mater.,* 2013, **23**, 2736.
8 L. Etgar, W. Zhang, S. Gabriel, S. G. Hickey, M. K. Nazeeruddin, A. Eychmüller, B. Liu and M. Grätzel, *Adv. Mater.,* 2012, **24**, 2202.
9 A. L. Linsebigler, G. Lu and J. T. Yates, *Chem. Rev.,* 1995, **95**, 735.
10 X. Pang, W. Chang, C. Chen, H. Ji, W. Ma and J. Zhao, *J. Am. Chem. Soc.,* 2014, **136**, 8714.
11 G. Fu, P. S. Vary and C. T. Lin, *J. Phys. Chem. B,* 2005, **109**, 8889.
12 R. Comparelli, E. Fanizza, M. L. Curri, P. D. Cozzoli, G. Mascolo, R. Passino and A. Agostiano, *Appl. Catal. B-Environ.,* 2005, **55**, 81.
13 F. Pan, J. Zhang, W. Zhang, T. Wang and C. Cai, *Appl. Phys. Let.,* 2007, **90**, 122114.
14 J. M. Jung, M. Wang, E. J. Kim, C. Park and S. H. Hahn, *Appl. Catal. B- Environ.,* 2008, **84,** 389.
15 S. Ghazi, A. Sayigh and K. Ip, *Sust. Energ. Rev.,* 2014, **33**, 742.
16 J. W. Leem, J. S. Yu, J. Heo, W. K. Park, J. H. Park, W. J. Cho and D.E. Kim, *Sol. Energ. Mater. Sol. C.,* 2014, **120**, 555.
17 J. D. Rancourt, *Optical thin Films: Users Handbook*, McGraw-Hill, New York, 1987.
18 S. Nobuyuki, F. Akira, W. Toshiya and H. Kazuhito, *J. Phys. Chem. B,* 2003, **107**, 1028.
19 F. Razan, D. Ralf and B. Detlef, *Langmuir*, 2013, **29**, 3730.
20 K. Hashimoto, H. Irie and A. Fujishima, *Jpn. J. Appl. Phys.*, 2005, **44**, 8269.
21 J. S. Kim, S. H. Hahn and E. J. Kim, *J. Korean Phys. Soc.*, 2007, **51**, 2014.
22 H. Sankur and W. Gunning, *J. Appl. Phys.*, 1989, **66**, 4747.
23 Z. L. Hua, J. L. Shi, L. X. Zhang, M. L. Ruan and J. N. Yan, *Adv. Mater.*, 2002, **14**, 830.
24 J. Jun, J. H. Shin and M. Dhayal, *Appl. Surf. Sci.*, 2006, **252**, 3871.
25 V. Levitcharsky, R. G. Saint-Jacques, Y. Q. Wang, L. Nikolova, R. Smirani and G. G. Ross, *Surf. Coat. Tech.*, 2007, **201**, 8547.
26 C. Anderson and A. J. Bard, *J. Phys. Chem. B*, 1997, **101**, 2611.
27 T. Sekiya, S. Kamel and S. Kurita, *J. Lumin.*, 2000, **87-89**, 1140.
28 D. J. Kim, S. H. Hahn, S. H. Oh and E. J. Kim, *Mater. Let.,* 2002, **57,** 355.